FIBRE-REINFORCED CONCRETE UNDER UNIAXIAL TENSILE LOADING

Jyrki Kullaa
Lic.Tech. (M.Sc.) Research Scientist
VTT Building Technology
Kemistintie 3
FIN-02150 ESPOO
FINLAND

ABSTRACT

The mechanics of fibre-reinforced concrete under uniaxial loading is studied. The main part of the study considers the behaviour after cracking.

A new constitutive model is developed. It takes into account also the strain-softening part of the stress-strain curve. In addition, the crack spacing and the crack width are calculated. The fibres are smooth and flexible. They can be short or continuous, aligned or randomly distributed, brittle or ductile, hard or soft. Moreover, different types of fibres may lie in the same matrix. The model takes into account single-fracture or multiple-cracking states and different fracture mechanisms: fibre fracture or pull-out.

The results of the new model are promising. The effects of different parameters can be studied and even new formulas can be found. The model can also be used in the design of composite materials.

Key words: fibre reinforcement, constitutive model, cracking, tensile stress

1 INTRODUCTION

Fibre reinforcement has been shown to improve the tensile behaviour of concrete. With just a few percent of fibres the toughness increases, and with a larger amount of fibres the tensile strength also increases. In FRC composites, the major effect of the fibres is noted in the post-cracking case, where the fibres bridge across the cracked matrix /3/.

The composite may fail in a single-fracture mode or if the fibre volume content is high, it is possible to reach the multiple-cracking stage of the matrix. In the single-fracture mode the bridging of fibres across the crack to transfer the load is usually simulated by pull-out tests, but in the multiple-cracking mode the simulation is no longer possible, while the force distribution in the fibre between the cracks is no more similar to the pull-out test.

Wang /7/ developed a theoretical statistical model to predict the stress–strain curve of fibre-reinforced concrete in the single-fracture mode. The bond was assumed to be constant frictional. The fibres are in a 3-dimensional random distribution.

The stepwise linear ACK model /1/ predicts the stress-strain behaviour in the multiple- and post-multiple-cracking stages. The model takes into account the fibre length and orientation by efficiency factors. The strain softening region is not included in the ACK model.

2 A NEW CONSTITUTIVE MODEL

The new proposed model takes into account the single-fracture or multiple-cracking states and different fracture mechanisms: fibre fracture or pull-out. The fibres are assumed to be mutually independent. They may be short or continuous, aligned or randomly distributed, brittle or ductile, hard or soft. Moreover, different types of fibres may lie in the same matrix (hybrid fibre composite). The fibres are supposed to carry only axial tensile stress. The bending effect and the concentrated friction force at the fibre exit point are neglected.

The constitutive model is strain-controlled: The strain is increased monotonously and the corresponding composite stress is evaluated. Thus also the strain-softening part of the stress-strain curve can be taken into account.

The crack is assumed to initiate when the matrix stress or strain reaches the critical value, σ_{mu} or ϵ_{mu}, respectively. In the multiple-cracking state the initial crack spacing is chosen to be half of the length of the longest fibre type. At more advanced stages of loading, new cracks are assumed to initiate between the already-existing cracks so that the crack spacings are equal. The crack widths are supposed also to be equal.

Assuming that the fibres are mutually independent, the contribution of the fibres may be superposed. For example, in hybrid reinforcement different types of fibres can be analysed separately or fibres with different embedded lengths may be averaged.

The stress of the composite can be evaluated by

$$\sigma_c = \sum_{i=1}^{n} V_{fi}\overline{\sigma_{fi}} \tag{1}$$

where n is the number of different fibre types, V_{fi} is the fibre volume content of one fibre type and $\overline{\sigma_{fi}}$ is the average stress carried by a fibre of one type.

2.1 Uncracked composite

Before cracking, the behaviour is assumed to follow the rules of mixtures:

$$\sigma_c = \left(E_m V_m + \sum \eta_l \eta_\theta E_f V_f\right) \epsilon_c \tag{2}$$

where ϵ_c is the strain of the composite, E_m and E_f are the moduli of elasticity of the matrix and the fibre, respectively, V_m and V_f ($V_m = 1 - \sum V_f$) are the volume contents of the matrix and the fibre, respectively, and η_l and η_θ are the efficiency factors of fibre length and orientation, respectively, in the uncracked stage.

The first crack is initiated when the composite strain reaches the critical value, ϵ_{cu}.

2.2 Single fracture

After the first crack, the situation in the vicinity of the crack can be modelled by the pull-out of fibres of different lengths and orientations simultaneously. The uncracked composite is modelled by the rules of mixtures.

The stress of the composite is

$$\sigma_c = \sum V_f \overline{\sigma_f(l,\theta)} \tag{3}$$

where l is the fibre embedded length and θ is the fibre orientation angle.

The detailed derivation of the following theory can be found elsewhere /4/. Only the summary is presented here.

Let us assume that the fibres are randomly oriented over the angle interval from θ_1 to θ_2 measured from the direction of the external load.

The average stress in the fibre can be evaluated from

$$\overline{\sigma_f} = \frac{1}{C}\frac{2}{l_f}\int_0^{l_f/2}\left[\int_C \sigma_f(l,\theta)\cos\theta dC\right] dl \tag{4}$$

where C represents either the area of the spherical surface A for a 3-dimensional distribution or the arc-length s for a 2-dimensional fibre distribution.

If we assume that the fibres are perfectly flexible, the fibre stress does not depend on the fibre orientation in the single-fracture mode. The average fibre stress can now be evaluated from

$$\overline{\sigma_f} = \eta_\theta \frac{2}{l_f}\int_0^{l_f/2}\sigma_f(l)dl \tag{5}$$

For a 3-dimensional distribution

$$\eta_\theta = \frac{\sin^2\theta_2 - \sin^2\theta_1}{2(\cos\theta_1 - \cos\theta_2)} \tag{6}$$

For a 2-dimensional distribution

$$\eta_\theta = \frac{\sin\theta_2 - \sin\theta_1}{\theta_2 - \theta_1} \tag{7}$$

For randomly distributed fibres ($\theta_1 = 0, \theta_2 = \pi/2$), the fibre orientation efficiency factors η_θ in 3- and 2-dimensional distributions are $1/2$ and $2/\pi$, respectively. Moreover, according to L'Hôpital's rule the factor for parallel fibres is $\cos\theta$ in both cases.

In the multiple-cracking state, the orientation efficiency factors obtained above can no longer be used, while the fibre stress depends also on the orientation of the fibres. The general Equation 4 should be used in the case of multiple cracking.

The stress and strain of the composite are

$$\sigma_c = \sum V_f \overline{\sigma_f(l,\theta)} = \sum \eta_\theta V_f \overline{\sigma_f(l)} \tag{8}$$

$$\epsilon_c = \frac{\sigma_c}{V_m E_m} + \frac{w}{L} \tag{9}$$

where L is the length of the test specimen, w is the crack width which can be calculated by summing the displacements of the fibre on both sides of the crack.

$$w = \Delta_1 + \Delta_2 \tag{10}$$

$$\Delta_1 = \Delta_1(P, l) \tag{11}$$

$$\Delta_2 = \Delta_2(P, l_f - l) \tag{12}$$

Δ_1 and Δ_2 are the displacements of the shorter and longer fibre embedded lengths, respectively. l is the shorter embedded length and l_f is the length of the fibre. The relation $\Delta_1(P,l)$ can be obtained by pull-out tests of different fibre embedded lengths, or by one pull-out test from which the bond parameters are obtained and using a theory in deriving the pull-out curves for different fibre embedded lengths. In this study the theory of Naaman et al. /5/ is used.

2.3 Multiple cracking

If the fibre content is sufficiently high, it is possible that the load-bearing capacity of the fibres is greater than the load on the composite at the first crack. Additional loading will result in additional cracks, until the matrix is divided into a number of segments, separated by cracks. The cracking stops when the stress transferred to the matrix no longer exceeds the cracking stress.

For simplicity, constant frictional stress transfer between fibres and matrix is assumed. It is also assumed that the crack spacings of different cracks are equal and that the crack widths of different cracks are also equal.

When the normal force of the fibre at the crack is P, the fibre displacement at the crack can be evaluated as follows. The local tensile force F in the fibre is

$$F(x) = P - t_f x \tag{13}$$

where t_f is the shear flow at the fibre-matrix interface. It is the product of the shear stress and the perimeter of the fibre: $t_f = \tau_f \psi$. x is the distance from the crack.

Let us assume that the matrix carries the transferred force with the area A_m. The strain difference between the fibre and the matrix is

$$\epsilon_f - \epsilon_m = \frac{F(x)}{A_f E_f} - \frac{P - F(x)}{A_m E_m} = \frac{P - t_f x}{A_f E_f} - \frac{t_f x}{A_m E_m} \tag{14}$$

The displacement of the fibre at the crack is evaluated by

$$\Delta = \int_0^c (\epsilon_f - \epsilon_m) dx = \frac{Pc}{A_f E_f} - \frac{1}{2} t_f c^2 \left(\frac{1}{A_m E_m} + \frac{1}{A_f E_f} \right) \tag{15}$$

where c is the distance from the crack where the fibre carries tension.

Fibres whose shorter embedded length is less than $l_x/2$ will slip. For constant frictional stress transfer, $l_x/2$ can be calculated from

$$\frac{l_x}{2} = \frac{P}{t_f} \tag{16}$$

Substituting $c = P/t_f$ in Equation 15, solving P/t_f, and taking the Equation 16 into account, leads to

$$\frac{l_x}{2} = \sqrt{\frac{2\Delta}{t_f} \left(\frac{1}{A_f E_f} - \frac{1}{A_m E_m} \right)^{-1}} \tag{17}$$

Let l be the fibre embedded length. For clarity, let us first assume that the fibres are aligned and perpendicular to the cracks. The effect of the fibre orientation can also be taken into account /4/. Futhermore, it is assumed that there exists a symmetrical fibre at the neighbouring crack with respect to the fibre being studied (see Figure 1). The crack spacing is $2s$. In Figure 1 on the left-hand side the tensile forces in the fibre and its symmetry fibre between two cracks are shown. The end of the line represents the fibre end. On the right-hand side the normal forces of the two fibres between the cracks are superposed for producing simpler formulas. The arrow represents the fibre force acting at the crack.

There are several force-transferring cases. Only one of them is represented here. The others can be found elsewhere /4/.

- If $l > l_x/2$

  $a = 2s - \frac{1}{2}(l - l_x/2)$

  a is the distance of the intersection point from the crack, as shown in Figure 1.

  - If $a > l_x/2$, the fibre slips at the neighbouring crack. The force is totally transferred to the matrix (Figure 1).

$$c = l_x/2 \tag{18}$$
$$h_1 = \min(2s - c, l_x/2) \tag{19}$$
$$h_2 = \min(l - 2s, l_x/2) \tag{20}$$

where h_1 and h_2 are the distances from the crack where the superposed forces become constant. Their values are needed in calculating the stress and strain of the matrix.

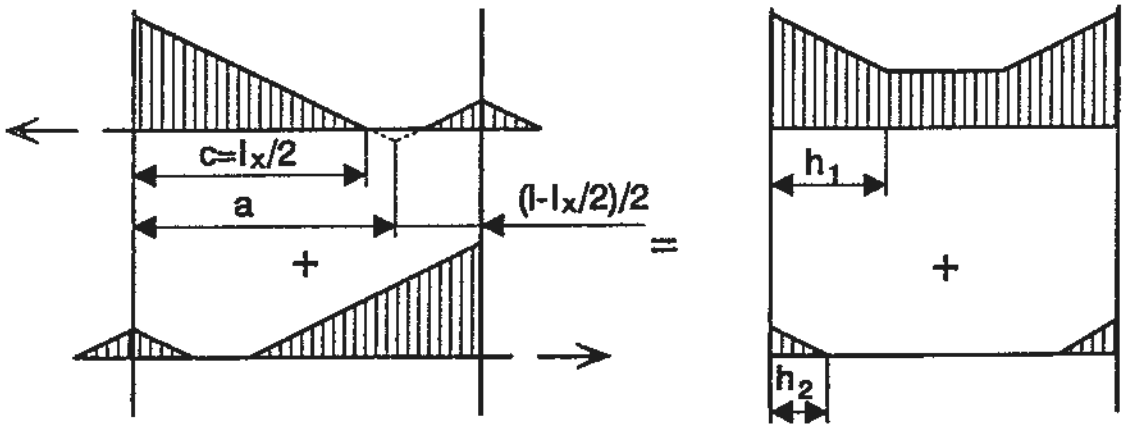

Figure 1. $2s - \frac{1}{2}(l - l_x/2) > l_x/2$. *The fibre slips at the neighbouring crack. The force is totally transferred to the matrix.* $c = l_x/2$, $h_1 = \min(2s - c, l_x/2) = 2s - c$, $h_2 = \min(l - 2s, l_x/2) = l - 2s$.

The force carried by the fibre at the crack can be solved from Equation 15:

$$P = \frac{A_f E_f}{c}\Delta + \frac{1}{2}t_f c\left(1 + \frac{A_f E_f}{A_m E_m}\right) \tag{21}$$

The crack width is found by summing the fibre displacements of both embedded lengths.

Because of new possible cracks, the stress or strain in the matrix between the cracks must be studied. In addition, the average strain in the matrix is calculated.

The strain of the matrix is evaluated by

$$\epsilon_m = \frac{\sigma_m}{E_m} = \frac{T(x)}{A_m E_m} = \frac{P - F(x)}{A_m E_m} \tag{22}$$

where σ_m is the stress of the matrix, and $T(x)$ is the normal force transferred to the matrix. The average force is

$$\overline{T(x)} = \frac{1}{s}\int_0^s T(x)dx \tag{23}$$

If ϵ_m exceeds the cracking strain, a new crack may initiate in the point where the excess occurs. The maximum strain is always in the middle of the matrix between the existing cracks, so the crack spacing is halved.

Let us examine the forces transferred from fibres with different embedded lengths. Figure 2 shows that fibre embedded lengths from 0 to $l_f/2 + s$ must be studied. The longer fibres are symmetry fibres.

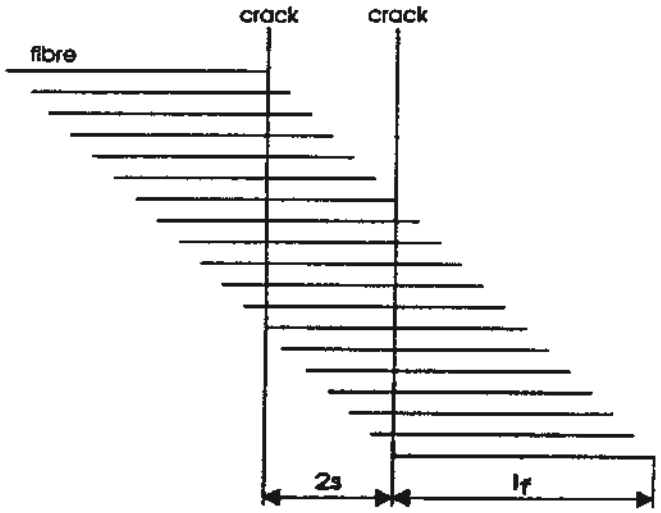

Figure 2. The distribution of fibres between two cracks.

There are three possible cases for the stress transfer. The formulas for only one of them is presented here. The other two can be found elsewhere /4/.

1. $l > 2s$.

   The fibre and its symmetry fibre overlap between the cracks.

   $h_2 \leq h_1$.

$$T(x) = \begin{cases} 2t_f x, & 0 \leq x \leq h_2 \\ t_f(x + h_2), & h_2 \leq x \leq h_1 \\ t_f(h_1 + h_2), & h_1 \leq x \leq s \end{cases} \tag{24}$$

$$T(s) = \begin{cases} 2t_f s, & h_2 > s \\ t_f(s + h_2), & h_1 > s \\ t_f(h_1 + h_2), & h_1 < s \end{cases} \tag{25}$$

$$\overline{T(x)} = \begin{cases} t_f s, & h_2 > s \\ \frac{1}{s}t_f\left(\frac{1}{2}s^2 - \frac{1}{2}h_2^2 + h_2 s\right), & h_1 > s \\ \frac{1}{s}t_f\left(-\frac{1}{2}h_1^2 - \frac{1}{2}h_2^2 + h_1 s + h_2 s\right), & h_1 < s \end{cases} \tag{26}$$

2. $l < s$ or $s > l_s/2$.

   The fibre and its symmetry fibre or their normal forces do not overlap between the cracks.

3. $s < l_s/2$ and $s < l \leq 2s$.

   The fibre and its symmetry fibre and their normal forces partially overlap between the cracks.

The average force in the middle of the matrix between the cracks is

$$\overline{T(s)} = \frac{1}{l_f}\int_0^{l_f} T(s)dl \tag{27}$$

and the average matrix strain can be evaluated by

$$\overline{\epsilon_m} = \frac{1}{l_f}\frac{1}{A_m E_m}\int_0^{l_f} \overline{T(x)}dl \tag{28}$$

The formulas are also valid for long fibres that extend over several cracks. The stress and strain of the composite can be evaluated by

$$\sigma_c = V_f\overline{\sigma_f(l,\theta)} \tag{29}$$

$$\epsilon_c = \overline{\epsilon_m} + \frac{w}{2s} \tag{30}$$

It can be seen that in the multiple-cracking stage the strain is no longer dependent on the specimen length, as it is in the single-fracture mode.

The formulas in the multiple-cracking stage for the composite with oriented fibres are presented elsewhere /4/.

3 EXAMPLES

3.1 The effect of different parameters

The stress-strain curves of different FRC composites in tension are evaluated and the effect of different parameters are studied. One parameter is varied at a time. The parameters of the basic material are: the fibre volume content $V_f = 0.03$, the length of the fibre $l_f = 30$ mm, the fibre diameter $d = 0.5$ mm, the specimen width $L = 50$ mm, the modulus of elasticity of the matrix $E_m = 21$ GPa, the matrix cracking stress $\sigma_{mu} = 3$ MPa, the modulus of elasticity of the fibre $E_f = 207$ GPa, the ultimate strength of the fibre $\sigma_{fu} = 1$ GPa, and the coefficient of friction $\mu = 0.6$. The following parameters are for modelling the fibre pull-out (see /5/). The Poisson ratio of the matrix $\nu_m = 0.35$, the Poisson ratio of the

fibre $\nu_f = 0.3$, the bond modulus $\kappa = 10^{13}$ N/m^3, the bond strength $\tau_{max} = 2.8$ MPa, the frictional bond shear stress $\tau_f = 2.5$ MPa, and the constants in modelling the decreasing friction $\xi = -0.01$ and $\eta = 0.2$. The fibres are 3-dimensionally randomly distributed. The fibres are assumed to break when the stress in a fibre exceeds σ_{fu}.

The diameter of the fibre d is varied from 0.05 mm to infinity and the length of the fibre l_f is varied from 0 to 300 mm, so that the effect of the aspect ratio l_f/d can be studied. The calculations show that it makes no difference whether the fibre length is increased or the fibre diameter is decreased. Figure 3 shows the effect of the aspect ratio on the stress-strain curve. It is seen that increasing the fibre length or decreasing the fibre diameter increase the strength and toughness until the fibres are so long or thin that they break.

The calculations are strain controlled, i.e. the strain of the composite is increased monotonously. Hence there are jumps in the multiple-cracking stage when new cracks are formed. The sharply descending curve with jumps represents the breaking of fibres.

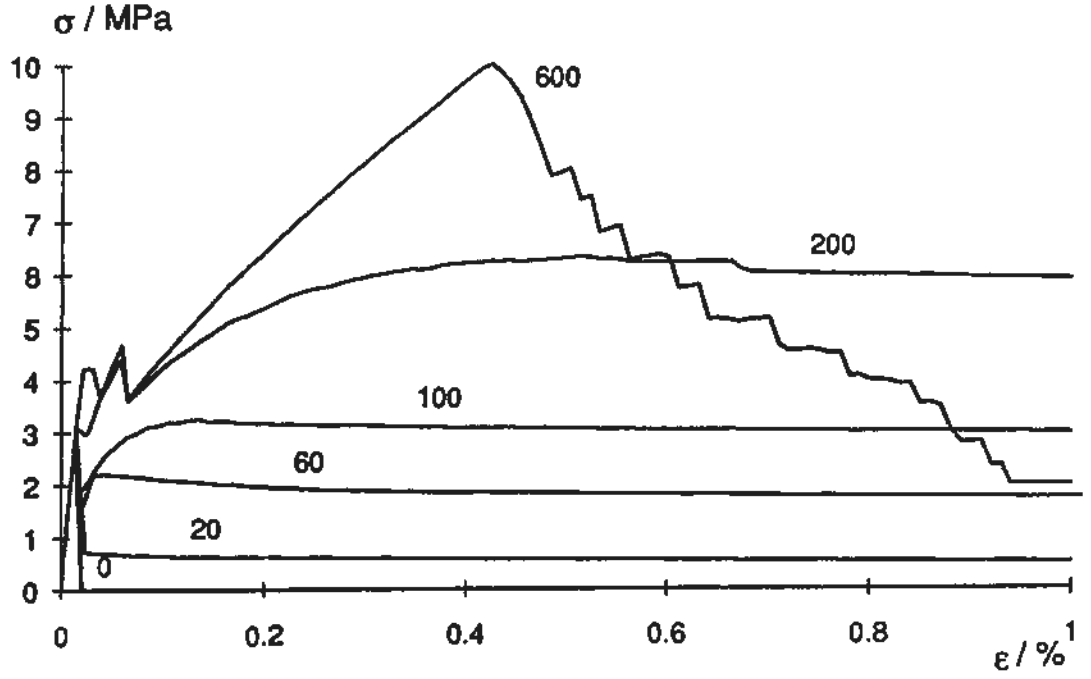

Figure 3. The effect of fibre aspect ratio on the constitutive relation.

In Figure 4 the effect of fibre content is shown. The fibre volume content of the present material must exceed 5 percent to strengthen the composite.

The effect of nylon fibres on steel-fibre-reinforced concrete is studied. The following properties according to Wang et al. /8/ are used. $d = 0.0176$ mm, $l_f = 38.1$ mm, $E_f = 5$ GPa, $\sigma_{fu} = 1$ GPa, $\tau = 0.16$ MPa. The elastic and frictional shear stresses are assumed to be equal, and the other pull-out parameters ν_f, μ κ, ξ and η are chosen to be the same as for steel fibres.

From Figure 5 it can be seen that by increasing the nylon fibres, the strength of the composite increases. More distinctly, the strain capacity and the toughness increase.

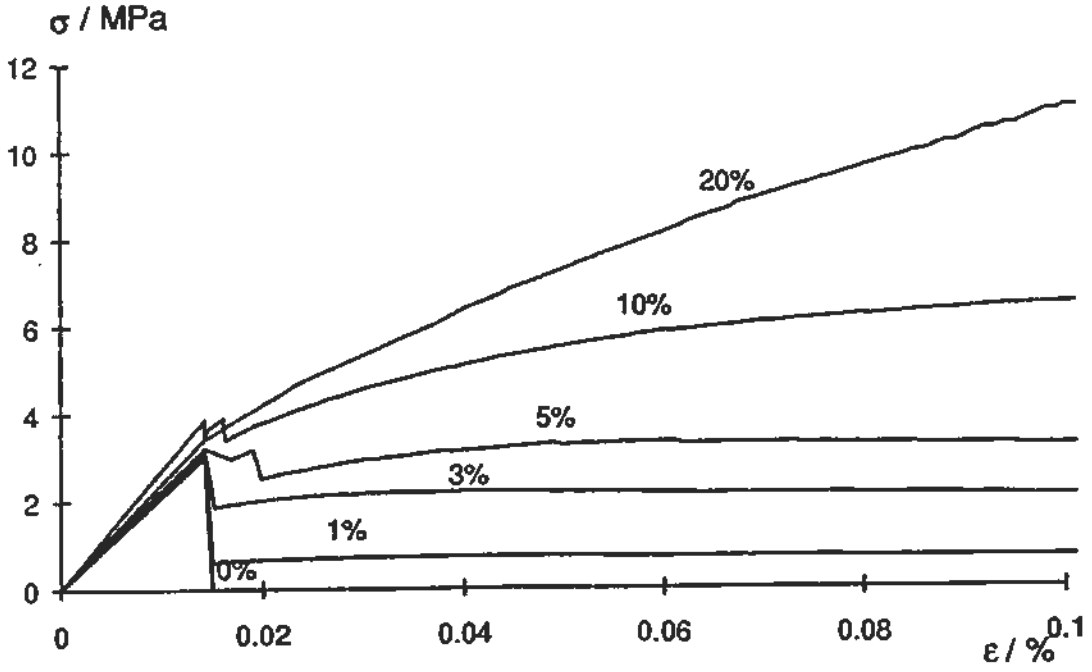

Figure 4. The effect of fibre volume content on the constitutive relation.

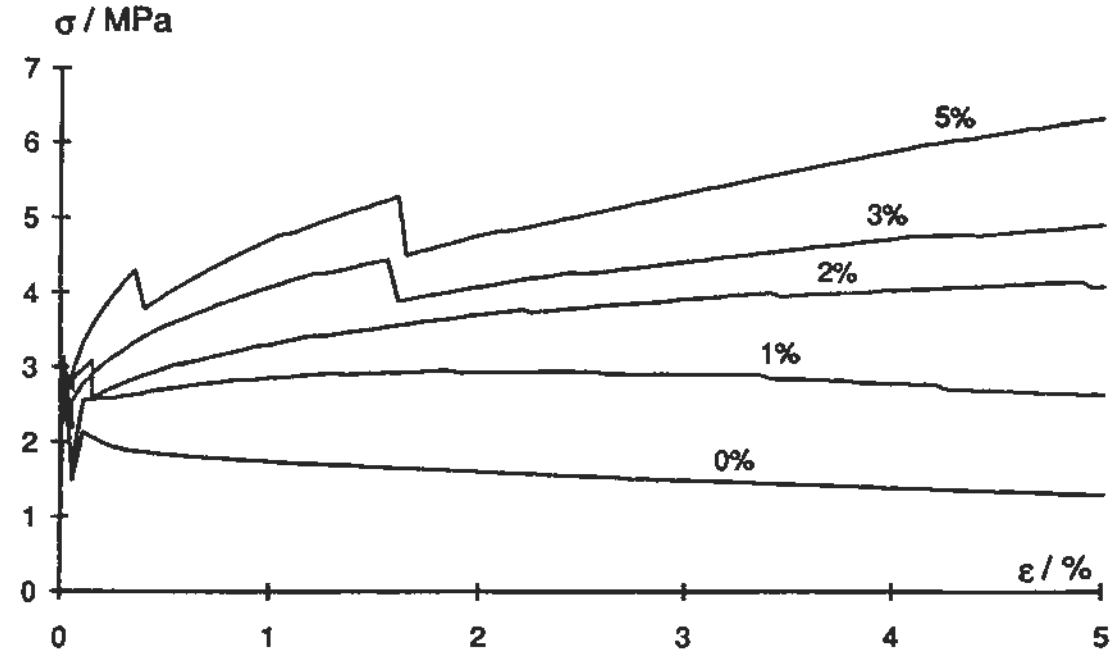

Figure 5. The effect of nylon fibre volume content on the constitutive relation of steel-fibre-reinforced concrete. The volume content of the steel fibres is 3 %.

3.2 Comparison of the model with the ACK model

The basic material of the previous section is chosen. If the fibres slip, the tensile strength of the composite according to the ACK model is

$$\sigma_{cu} = \eta_\theta V_f \tau_f \frac{l_f}{d} \tag{31}$$

The fibre efficiency factor for randomly oriented fibres is $\eta_\theta = 0.5$. In Table 1 a comparison of the present and the ACK model is presented.

In Table 1 the mark (B) after the strength value means that a part of the fibres break instead of sliding. It can be seen that the present model gives lower values for the composite strength than the ACK model. Moreover, with a higher strength the relative difference is larger.

When the fracture mode is the fibre breakage, the strength of the composite and the crack spacing are examined. According to the ACK model /2/ the minimum crack spacing for a composite with short, aligned fibres is

$$x_d = \frac{l_f - \sqrt{l_f^2 - 4 l_f x}}{2} \tag{32}$$

where x is the minimum crack spacing for continuous fibres:

$$x = \frac{V_m}{V_f} \frac{\sigma_{mu} d}{4\tau_f} \tag{33}$$

σ_{mu} is the matrix cracking stress. The crack spacing is between x_d and $2x_d$.

The strength of the composite is evaluated by

$$\sigma_{cu} = \left(1 - \frac{l_c}{l_f}\right) \sigma_{fu} V_f \tag{34}$$

where

$$l_c = \frac{\sigma_{fu} d}{4\tau_f} \tag{35}$$

In the calculations, several composites were analyzed. It could be seen that the present model is in a good agreement with the ACK model for composites with short, aligned fibres /4/.

Table 1. Comparison of the tensile strength between the ACK model and the new model when the fracture mode is fibre sliding. The mark (B) after the strength value means that a part of the fibres break instead of sliding.

d / mm		ACK model $\eta_\theta V_f \tau_f l_f / d$ / MPa	New model σ_{cu} / MPa	Relative diff. / %
∞		0	0	0
1.5		0.75	0.75	0
0.5		2.25	2.22	-1.33
0.3		3.75	3.30	-12.0
0.15		7.50	6.47 (B)	-13.7
0.05		22.5	10.1 (B)	-55.1
V_f / %				
0		0	0	0
1		0.75	0.74	-1.33
3		2.25	2.22	-1.33
5		3.75	3.36	-10.4
10		7.5	6.63	-11.6
20		15	13.6	-9.33
τ_f / MPa				
0		0	0	0
2		1.80	1.77	-1.67
4		3.60	3.18	-11.7
6		5.40	4.73	-12.4
8		7.20	6.21	-13.8
12		10.8	8.11 (B)	-24.9
θ	η_θ			
0	1	4.5	4.13	-8.22
30	0.866	3.90	3.59	-7.95
60	0.5	2.25	2.22	-1.33
90	0	0	0	0
2-D				
0–30	0.955	4.3	3.95	-8.14
0–60	0.827	3.7	3.42	-7.57
0–90	0.637	2.9	2.82	-2.76
3-D				
0–30	0.933	4.2	3.85	-8.33
0–60	0.75	3.38	3.23	-4.44
0–90	0.5	2.25	2.22	-1.33

The crack spacing and the composite strength were calculated also for composites with randomly oriented short fibres. The results were compared to the equations presented above to check if there is a correlation between the present model and the calculated values for short, aligned fibres.

The analysis showed that for composites with randomly oriented short fibres the following equations can be used /4/.

$$x_d = \frac{1}{\eta_\theta} \frac{l_f - \sqrt{l_f^2 - 4 l_f x}}{2} \tag{36}$$

and

$$\sigma_{cu} = \eta_\theta \left(1 - \frac{l_c}{l_f}\right) \sigma_{fu} V_f \tag{37}$$

where the fibre orientation efficiency factor is $\eta_\theta = 0.375$.

4 CONCLUDING REMARKS

A statistical model of the tensile constitutive relation of fibre-reinforced concrete was established. The model takes into account both the single-fracture and multiple cracking.

The modelling of the single-fracture mode is based on the fibre pull-out. The pull-out model used in this study is based on the model of Naaman et al. /5/. It includes the elastic and frictional shear stresses, the contribution of matrix deformation and the decaying of the frictional stress transfer.

The cracks are supposed to initiate when the matrix stress or strain reaches the critical values, σ_{mu} or ϵ_{mu}, respectively. However, according to Shah /6/, the cracking strength of the matrix increases with increasing fibre content. Therefore, a fracture mechanics approach to the criteria of cracking should be developed.

In the multiple cracking, constant frictional stress transfer is assumed. It is assumed that every fibre has a so-called symmetry fibre that carries the load in the neighbouring crack. The average values are evaluated from effects of fibres with different orientations and embedded lengths.

In the single-fracture mode, the strain depends on the specimen length, unlike in the case of the multiple-cracking stage.

It was seen that in the multiple-cracking stage the orientation efficiency factor for randomly oriented short fibres was not 1/2 as obtained by Equation 6. Instead, it was found to be about 0.375.

The new proposed model can be used in designing and tailoring new FRC composites. In addition, it can be used in analysing structures, e.g. beams. The model may also be applied to other brittle matrix composites, e.g. ceramics.

5 ACKNOWLEDGEMENTS

This study is part of the research programme "Composite Materials and Structures in the Construction Industry" 1990–1992 and was supported by the Technical Research Centre of Finland.

6 REFERENCES

/1/ Aveston, J., Cooper, G. A. & Kelly, A. 1971. Single and multiple fracture. The Properties of Fibre Composites. Proc. Conf. National Physical Laboratories. 4 Nov. 1971. Guildford. IPC Science and Technology Press Ltd. Pp. 15–24.

/2/ Aveston, J., Mercer, R. A. & Sillwood, J. M. 1974. Fibre reinforced cements – scientific foundations for specifications. Composites – standards, testing and design. Conference Proceedings National Physical Laboratory. IPC Science and Technology Press, Guildford. Pp. 93–103.

/3/ Bentur, A. & Mindess, S. 1990. Fibre Reinforced Cementitious Composites. London. Elsevier Science Publishers Ltd. 449 p.

/4/ Kullaa, J. 1994. Constitutive modelling of fibre-reinforced concrete under uniaxial tensile loading. Composites. To be published.

/5/ Naaman, A.E., Namur, G.G., Alwan, J.M. & Najm, H.S. 1991. Fiber Pullout and Bond Slip. I: Analytical Study. Journal of Structural Engineering, Vol 117, No. 9. ASCE. pp. 2769–2790.

/6/ Shah, S. P. 1990. Toughening of Quasi-Brittle Materials due to Fibre Reinforcing. In: Shah, S. P. (edit.) Micromechanics of Failure of Quasi-Brittle Materials. London. Elsevier. Pp. 1–11.

/7/ Wang, Y. 1985. Mechanics of Fibre Reinforced Concrete. MSc Thesis. Department of Mechanical Engineering, Massachusetts Institute of Technology. 175 p.

/8/ Wang, Y., Backer, S. & Li, V.C. 1989. A statistical tensile model of fibre reinforced cementitious composites. Composites, Vol 20, No 3. Pp. 265–274.